

Extraction of the sub-bandgap density-of-states in polymer thin-film transistors with the multi-frequency capacitance-voltage spectroscopy

Jaeman Jang, Jaehyeong Kim, Minkyung Bae, Jaewook Lee, Dong Myong Kim et al.

Citation: *Appl. Phys. Lett.* **100**, 133506 (2012); doi: 10.1063/1.3698455

View online: <http://dx.doi.org/10.1063/1.3698455>

View Table of Contents: <http://apl.aip.org/resource/1/APPLAB/v100/i13>

Published by the [American Institute of Physics](#).

Related Articles

Threshold voltage modulation mechanism of AlGaN/GaN metal-insulator-semiconductor high-electron mobility transistors with fluorinated Al₂O₃ as gate dielectrics

Appl. Phys. Lett. **100**, 133507 (2012)

Positive-negative turbulence-free ghost imaging

Appl. Phys. Lett. **100**, 131114 (2012)

Polarization-induced remote interfacial charge scattering in Al₂O₃/AlGaN/GaN double heterojunction high electron mobility transistors

Appl. Phys. Lett. **100**, 132105 (2012)

1-nm-capacitance-equivalent-thickness HfO₂/Al₂O₃/InGaAs metal-oxide-semiconductor structure with low interface trap density and low gate leakage current density

Appl. Phys. Lett. **100**, 132906 (2012)

Second-harmonic generation reveals the oxidation steps in semiconductor processing

J. Appl. Phys. **111**, 064504 (2012)

Additional information on *Appl. Phys. Lett.*

Journal Homepage: <http://apl.aip.org/>

Journal Information: http://apl.aip.org/about/about_the_journal

Top downloads: http://apl.aip.org/features/most_downloaded

Information for Authors: <http://apl.aip.org/authors>

ADVERTISEMENT



ACCELERATE AMBER AND NAMD BY 5X.
TRY IT ON A FREE, REMOTELY-HOSTED CLUSTER.

LEARN MORE

Extraction of the sub-bandgap density-of-states in polymer thin-film transistors with the multi-frequency capacitance-voltage spectroscopy

Jaeman Jang,¹ Jaehyeong Kim,¹ Minkyung Bae,¹ Jaewook Lee,¹ Dong Myong Kim,¹ Dae Hwan Kim,^{1,a)} Jiyoul Lee,^{2,a)} Bang-Lin Lee,² Bonwon Koo,² and Yong Wan Jin²

¹*School of Electrical Engineering, Kookmin University, Jeongneung-dong, Seongbuk-gu, Seoul 136-702, Korea*

²*Display Device Laboratory, Samsung Advanced Institute of Technology, Yongin-si 446-712, Korea*

(Received 22 December 2011; accepted 12 March 2012; published online 30 March 2012)

The multi-frequency capacitance-voltage (C - V) spectroscopy is proposed for extracting the sub-bandgap density-of-states (DOS) of polymer semiconductors and demonstrated in three different thiophene-based organic thin-film transistors including poly(3-hexylthiophene), poly(3,3''-didodecylquaterthiophene), and poly(didodecylquaterthiophene-alt-didodecylbithiazole). The density of exponential tail and exponential deep states are extracted to be in the range of $3.0 \times 10^{18} \sim 1.5 \times 10^{19} \text{ cm}^{-3} \text{ eV}^{-1}$ and $3.0 \times 10^{16} \sim 3.0 \times 10^{17} \text{ cm}^{-3} \text{ eV}^{-1}$, respectively. The extracted DOS correspond to the polymer semiconductor-dependence of the measured crystallinity and mobility. In addition, the extracted DOS values are verified by comparing the measured I - V characteristics with the simulated results through a technology computer-aided design tool. © 2012 American Institute of Physics. [<http://dx.doi.org/10.1063/1.3698455>]

The sub-bandgap density-of-states (DOS) in organic films including small-molecule and polymer semiconductors are closely related to the stability and the device performance.¹ For example, key parameters of the device performance such as the field-effect mobility, threshold voltage, subthreshold swing, and electrical stability are considerably influenced by bulk trap states in the semiconductor or interface states between the semiconductor and the dielectric. Therefore, it is obvious that the accurate estimation of the sub-bandgap DOS in the organic semiconductor bulk or at the interface is of practical importance for the device performance enhancement. More importantly, the performance of organic semiconductor-based circuits and systems should be assessed with respect to the DOS-dependence of the small signal response under a specific bias point because the speed of circuitry is determined by the small signal response. To date, various techniques for extracting the DOS in organic thin-film transistors (TFTs) such as thermally stimulated current measurement,² ultraviolet photoelectron spectroscopy,³ the Meyer-Neldel rule method,⁴ and the photo-excited charge collection⁵ have been demonstrated. However, these techniques are somewhat destructive schemes and potentially mutilate the organic semiconductor films, because they are generally accompanied with the light illumination or thermal effects.⁶ More noticeably, the experimental techniques for directly extracting the DOS in the small signal capacitance of organic TFTs are rarely reported despite of these importance.

In this letter, as an efficient technique for extracting the sub-bandgap DOS of organic semiconductor directly from the small-signal capacitance characteristics of organic TFTs, the multi-frequency capacitance-voltage (C - V) spectroscopy is proposed and demonstrated for extracting the sub-bandgap DOS: $g(E)$ [$\text{cm}^{-3} \text{ eV}^{-1}$], near the valence band maximum (E_V) in a

variety of polymer semiconductors including regio-regular poly(3-hexylthiophene) (P3HT), poly(3,3''-didodecylquaterthiophene) (PQT-12),⁷ and poly(didodecylquaterthiophene-alt-didodecylbithiazole) (PQBTz-C12).⁸ As a significant merit, the multi-frequency C - V spectroscopy requires no special preparation or measurement setup (for the light illumination and/or thermal effects). The technique directly reflects the effects of $g(E)$ on the circuit performance because it uses the gate-to-source/drain (S/D) voltage-dependent small signal capacitances.

Fig. 1(a) schematically illustrates chemical structures of the polymer semiconductors used as active layers (P3HT, PQT-12, and PQBTz-C12) of organic TFTs which are well known materials potentially useful in the printed electronic applications. In order to investigate the crystalline quality of the individual polymer semiconductor, we conducted the x-ray diffraction (XRD) measurement using Cu $K\alpha$ ($\lambda = 1.5405 \text{ \AA}$). Fig. 1(b) displays the XRD spectra of the polymer semiconductor films obtained by the spin-coating onto the octadecyltrichlorosilane (ODTS)-treated SiO_2 substrates. As shown in these spectra, the PQBTz-C12 film has a high intensity with the 4th peak in the (h00) direction, while the P3HT film and the PQT-12 film have only the 3rd peak in the same direction. In addition, the d -spacing difference between PQT-12 (17.0 \AA) and P3HT (16.5 \AA) is only 0.5 \AA even though the alkyl-chain length of PQT-12 is two times longer than that of P3HT.⁹ It may lead us to speculate that the inter-digitation of the alkyl-side chain in the PQT-12 is more efficient than that in the P3HT and the PQT-12 film has more improved molecular ordering, which should affect the bulk trap density of the polymer semiconductor in organic TFTs.

For experimental investigation, we fabricated coplanar structured TFTs on a glass substrate as shown in Fig. 1(c). The fabrication process starts with a sputtered deposition of molybdenum (Mo) as the gate material. The deposited Mo was patterned by a conventional photo-lithography to form a

^{a)}Authors to whom correspondence should be addressed. Electronic addresses: drlife@kookmin.ac.kr and jiyoul.lee@samsung.com.

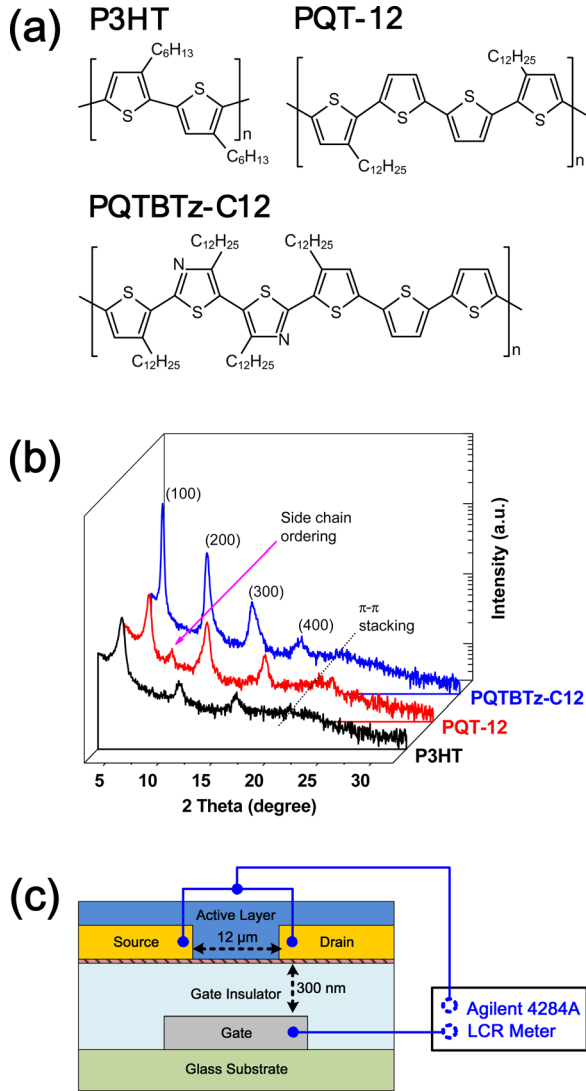


FIG. 1. (a) Schematic of chemical structures of the polymer TFTs. (b) XRD spectra of the 110 nm thick spin-coated P3HT, PQT-12, and PQTBTz-C12 polymer semiconductor films. (c) The cross-sectional view and the multi-frequency C - V measurement setup of the polymer TFT.

gate electrode. Then, the 300-nm-thick silicon dioxide (SiO_2) was deposited by the plasma enhanced chemical vapor deposition (PECVD) method as a gate dielectric layer ($T_{\text{ox}} = 300 \text{ nm}$). Then, gold (Au) was deposited by the e-beam evaporator and photo-lithographically patterned to serve as source and drain electrodes. The channel width (W) and length (L) were $120 \mu\text{m}$ and $12 \mu\text{m}$, respectively. The surface of the gate insulator was treated with a self-assembled monolayer (SAM) of ODTS (purchased from Aldrich). Polymer semiconductors were dissolved in tetrahydronaphthalene (THN) at a concentration of 0.2 wt. % and then ink-jet printed via Dimatix printer. Finally, the channel polymer films were cured at an appropriate temperature (140°C for P3HT (Purchased from Aldrich), 130°C for PQT-12 (Purchased from American Dye Source), and 175°C for PQTBTz-C12 (Synthesized in SAIT)) for 1 h in N_2 ambient. The thickness of all polymer films (T_{polymer}) was confirmed to be $\sim 30 \text{ nm}$ by the focused ion-beam scanning electron microscope (FIB-SEM).

Fig. 1(c) illustrates the measurement setup for the multi-frequency C - V spectroscopy, and its equivalent RC models

are shown in Figs. 2(a)–2(c). First of all, the extraction of $g(E)$ near E_V is demonstrated in the P3HT TFT starting from the frequency-dependent C - V measurement between the gate and S/D electrodes (the bias voltage is represented by V_{GS}) over a wide range of the small signal frequency as shown in Fig. 2(d), by using an a precision LCR meter (Agilent 4284 A). The proposed RC model is based on the postulation that the frequency-dependence of the measured C - V characteristic of organic TFTs is attributed to C_{LOC} (the capacitance component due to the V_{GS} -responsive localized charges: Q_{LOC} [trapped in the sub-bandgap DOS $g(E)$]), R_L (the equivalent resistance reflecting the $V_{\text{GS}}(t)$ -dependent retardation of $Q_{\text{LOC}}(t)$) [i.e., the resistance characterizing the frequency dispersion of the capture-emission process of holes localized in the sub-bandgap $g(E)$], and C_{FREE} (the capacitance component originated from the V_{GS} -responsive free hole charges: Q_{FREE} in the valence band ($E \leq E_V$)). Therefore, under this postulation, the physical situation of the C - V measurement in Fig. 1(c) is equivalent to the model shown in Fig. 2(c). We note that C_{OX} and R_S are the gate insulator capacitance and the extrinsic S/D series resistance in the C - V measurement, respectively. It is also assumed that all of C_{LOC} , C_{FREE} , and R_L are V_{GS} -dependent but independent of the small signal frequency (f or ω).

In the parallel-mode measurement by the LCR meter, the measured impedance Z_{meas} is marked in Fig. 2(a). Using Figs. 2(a) and 2(b), the intrinsic channel capacitance (C_{CH}) and the intrinsic channel resistance (R_{CH}) can be calculated from Z_{meas} , R_S , and C_{OX} as described in Eqs. (1) and (2)

$$R_{\text{CH}} = \sqrt{\frac{C_M(1 + D_M^2) - C_{\text{OX}}}{\omega^2 C_{\text{CH}}^2 C_{\text{OX}} - \omega^2 C_{\text{CH}} C_M (1 + D_M^2) (C_{\text{CH}} + C_{\text{OX}})}}; \quad (1)$$

$$D_M = \frac{1}{\omega C_M R_M},$$

$$C_{\text{CH}} = \frac{bC_{\text{OX}}^2 - b^2C_{\text{OX}}}{\{(ab\omega)^2 + 1\}C_{\text{OX}}^2 - 2bC_{\text{OX}} + b^2};$$

$$a = \frac{D_M}{\omega C_M (1 + D_M^2)} - R_S, \quad b = C_M (1 + D_M^2). \quad (2)$$

By de-embedding C_{OX} and R_S from Z_{meas} in Figs. 2(b) and 2(c), the intrinsic channel impedance (Z_{INT}) and the physical impedance of the polymer thin-film (Z_{polymer}) can be derived through Eqs. (3) and (4)

$$Z_{\text{INT}} = \frac{R_{\text{CH}}}{1 + (\omega C_{\text{CH}} R_{\text{CH}})^2} - \frac{j\omega C_{\text{CH}} R_{\text{CH}}^2}{1 + (\omega C_{\text{CH}} R_{\text{CH}})^2}, \quad (3)$$

$$Z_{\text{polymer}} = \frac{C_{\text{LOC}}^2 R_L^2}{\omega^2 C_{\text{LOC}}^2 C_{\text{FREE}}^2 R_L^2 + (C_{\text{LOC}} + C_{\text{FREE}})^2} - j \frac{\omega^2 C_{\text{LOC}}^2 C_{\text{FREE}} R_L^2 + (C_{\text{LOC}} + C_{\text{FREE}})}{\omega^3 C_{\text{LOC}}^2 C_{\text{FREE}}^2 R_L^2 + \omega (C_{\text{LOC}} + C_{\text{FREE}})^2}, \quad (4)$$

R_S under a fixed V_{GS} is extracted from the high frequency limit of the magnitude of Z_{meas} as indicated by the inset of Fig. 2(e), while C_{OX} is calculated from the dielectric

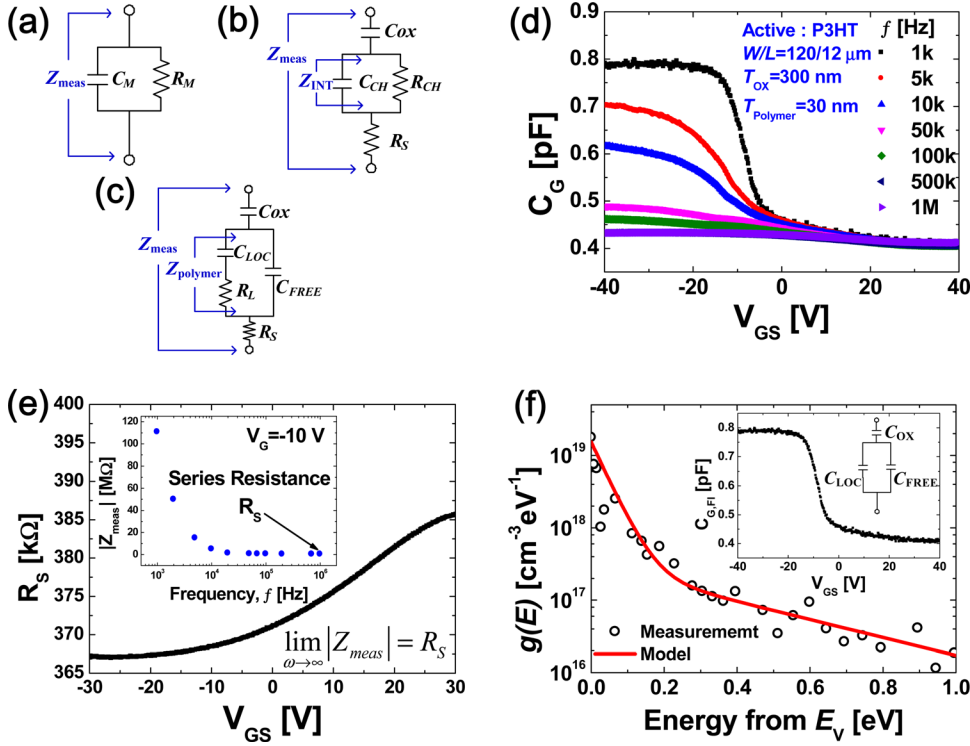


FIG. 2. (a) 2-element capacitance model for the parallel-mode C - V measurement. (b) 4-element capacitance model for de-embedding C_{OX} and R_S . (c) Physics-based gate capacitance model of organic TFTs. (d) The f -dependent C - V characteristics measured by an LCR meter. (e) The extracted V_{GS} -dependent R_S obtained from the high frequency $|Z_{meas}|$ in the 2-element model under a fixed V_{GS} as shown in the inset. (f) Extracted sub-bandgap DOS $g(E)$. The sub-bandgap energy level E is mapped through the relation of V_{GS} and ϕ_S with $C_{G,FI}(V_{GS})$ (in the inset) and Eq. (8).

constant and the size of the TFT device. In this way, $R_S(V_{GS})$ is extracted as seen in Fig. 2(e). Subsequently, using Z_{INT} [Fig. 2(b)] = $Z_{polymer}$ [Fig. 2(c)] with Eqs. (3) and (4), we

obtain C_{LOC} , C_{FREE} , and R_L . We also note that R_L is obtained through Eq. (5), and the condition of (6) is used for extracting $C_{LOC}(V_{GS})$ and $C_{FREE}(V_{GS})$.

$$R_L = \sqrt{\frac{\omega^2 C_{CH} R_{CH}^2 (C_{LOC} + C_{FREE})(C_{LOC} + C_{FREE} - C_{CH}) - (C_{LOC} + C_{FREE})}{\omega^2 C_{LOC}^2 C_{FREE} (1 + \omega^2 C_{CH} R_{CH}^2 (C_{CH} - C_{FREE}))}} \quad (5)$$

$$R_L(f_1) = R_L(f_2) = R_L(f_3). \quad (6)$$

Finally, the frequency-independent C_G - V_{GS} characteristic [$C_{G,FI}(V_{GS})$] is obtained as denoted by the inset of Fig. 2(f). We also note that $C_{LOC}(V_{GS})$ provides the information on the sub-bandgap DOS $g(E)$ over the C - V responsive energy range near E_V , and the $g(E)$ can be extracted by combining (7) and (8)

$$g(E) = g(V_{GS}) = g(\phi_S) = \frac{\Delta C_{LOC}}{q^2 \times W \times L \times T_{polymer}} = \frac{[C_{LOC}(V_{GS1}) - C_{LOC}(V_{GS2})]}{q^2 \times W \times L \times T_{polymer}}, \quad (7)$$

$$\phi_S = \int_{V_{FB}}^{V_{GS}} \left(1 - \frac{C_{G,FI}(V_{GS})}{C_{OX}} \right) dV_{GS}. \quad (8)$$

In our case, three frequencies ($f_1 = 1$ kHz, $f_2 = 100$ kHz, and $f_3 = 1$ MHz) were employed for the multi-frequency C - V spectroscopy. Finally, as indicated by the symbols in Fig. 2(f), $g(E)$ near E_V of P3HT is extracted. More importantly, the DOS model [fitted lines in Fig. 2(f)] is consistent with the well-known energy distribution of sub-bandgap DOS,

i.e., the superposition of exponential tail states: $g_{TD}(E)$ and exponential deep states: $g_{DD}(E)$ described by

$$g(E) = g_{DD}(E) + g_{TD}(E) = N_{DD} \times \exp\left(\frac{E_V - E}{kT_{DD}}\right) + N_{TD} \times \exp\left(\frac{E_V - E}{kT_{TD}}\right), \quad (9)$$

where $g_{DD}(E)$ is the deep part of $g(E)$ far away from E_V , $g_{TD}(E)$ is the tail part of $g(E)$ close to E_V , N_{DD} is the effective density of deep states, kT_{DD} is the characteristic energy of deep states, N_{TD} is the effective density of tail states, and kT_{TD} is the characteristic energy of tail states. The DOS model

TABLE I. Extracted parameters for sub-bandgap DOS $g(E)$ in polymer TFTs.

Extracted DOS parameters			
Parameters	P3HT	PQT-12	PQBTz-C12
N_{TD} [$\text{cm}^{-3} \text{eV}^{-1}$]	1.5×10^{19}	1.0×10^{19}	3.0×10^{18}
kT_{TD} [eV]	0.04	0.036	0.06
N_{DD} [$\text{cm}^{-3} \text{eV}^{-1}$]	3.0×10^{17}	2.0×10^{17}	3.0×10^{16}
kT_{DD} [eV]	0.35	0.35	0.70

parameters ($N_{TD} = 1.5 \times 10^{19} \text{ cm}^{-3} \cdot \text{eV}^{-1}$, $N_{DD} = 3.0 \times 10^{17} \text{ cm}^{-3} \cdot \text{eV}^{-1}$, $kT_{TD} = 0.04 \text{ eV}$, and $kT_{DD} = 0.35 \text{ eV}$) are also summarized in Table I.

Conclusively, for the P3HT-based TFTs, we can summarize all procedure of extracting $g(E)$ as follows. The frequency-sensitive nature of the measured C_G - V_{GS} characteristics in Fig. 2(d) can be modeled as the frequency dispersion of the RC network in Fig. 2(c), which consists of the frequency-independent RC components such as C_{OX} , C_{LOC} , C_{FREE} , R_L , and R_S . Then, we obtain $C_{LOC}(V_{GS})$ and translate it into $g(E)$ [as indicated in Eq. (7)] through a mapping to the sub-bandgap energy level via $C_{G,FI}(V_{GS})$ and Eq. (8). A detailed procedure of extracting $g(E)$ from the multi-frequency C - V spectroscopy was described in the example of inorganic counterpart.¹⁰ We note that the proposed approach provides a complicated nonlinear relationship between the surface potential (ϕ_s) and V_{GS} in a simple manner, with the aid of $C_{G,FI}(V_{GS})$ and Eq. (8). It means that the energy distribution of the extracted $g(E)$ is exactly matched with the sub-bandgap energy level of the polymer thin-films.

In order to verify the universality of the proposed approach, $g(E)$ is also extracted from PQT-12 and PQTBTz-C12 TFTs by the same procedure and model. In Fig. 3, we overlaid the $g(E)$ profiles of P3HT, PQT-12, and PQTBTz-C12 TFTs, which are obtained from the multi-frequency C - V spectroscopy of 3 polymer semiconductor TFTs. DOS parameters are also summarized in Table I. It should be noted that the polymer semiconductor with the superior crystallinity in Fig. 1(b) [PQTBTz-C12] clearly shows the lowest value of $g(E)$ and vice versa. From this result, we expect that the mobility of PQTBTz-C12 TFT is higher than those of two other TFTs. This is because with increased $g(E)$, i.e., N_{TD} , more holes should be spent for the Fermi-energy level to approach closer to E_V , which is followed by the mobility degradation under a fixed bias.

In order to quantitatively verify the extracted DOS, the DOS model in Table I is incorporated into the TCAD (technology computer-aided design) simulation, and the results (line) are compared with the measured transfer characteristics (symbol) in Fig. 4. In the symbols in Fig. 4, all TFTs show typical transistor behavior with a reasonable I_{ON}/I_{OFF} current ratio higher than 10^6 and with mobilities of $0.033 \text{ cm}^2/\text{Vs}$, $0.058 \text{ cm}^2/\text{Vs}$, $0.17 \text{ cm}^2/\text{Vs}$ for P3HT, PQT-12, and PQTBTz-C12, respectively. This observation in the

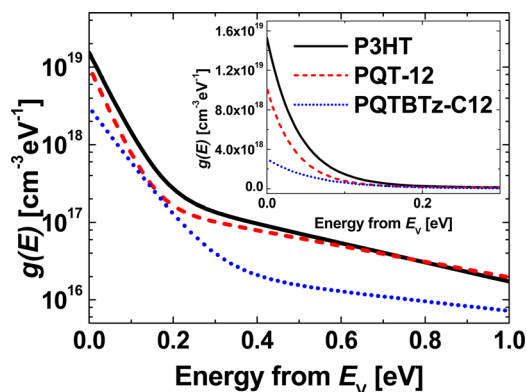


FIG. 3. The comparison of extracted $g(E)$ of the polymer TFTs (P3HT, PQT-12, and PQTBTz-C12). The inset shows $g(E)$ in a linear scale.

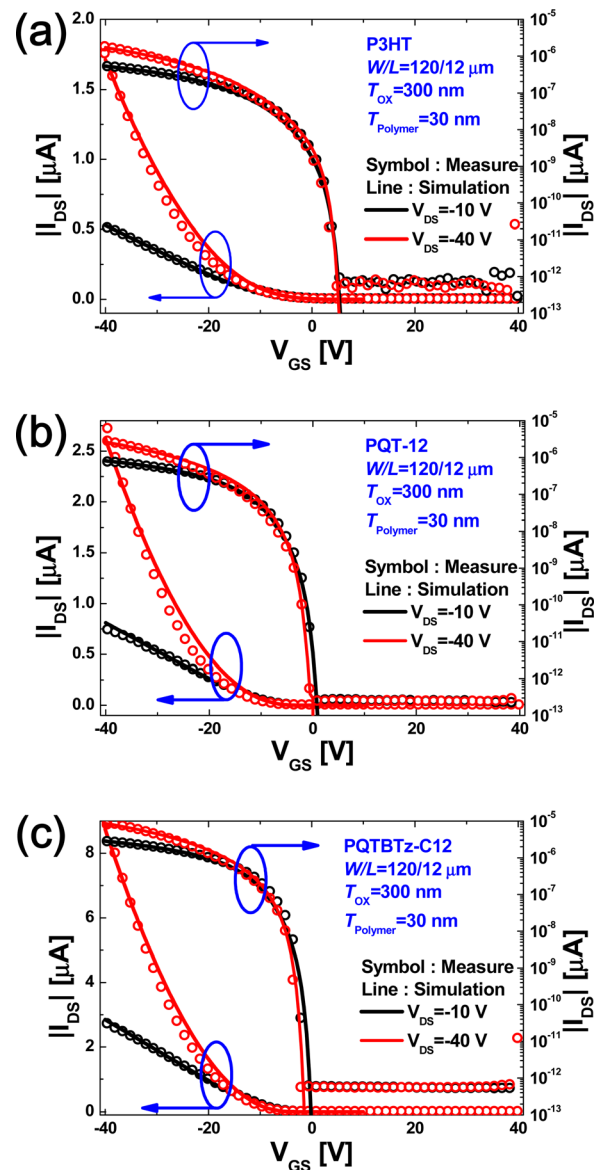


FIG. 4. Measured transfer characteristics of the polymer TFTs compared with the TCAD simulation result. (a) P3HT, (b) PQT-12, and (c) PQTBTz-C12.

polymer semiconductor-dependence of mobility agrees well with aforementioned DOS-based expectation. Most notably, in Fig. 4, the TCAD simulation results reproduce the measured I - V characteristics very well over a wide range of the drain-to-source bias (V_{DS}), which means that the proposed approach is quantitatively reasonable and potentially useful for the design of polymer semiconductor-based TFTs. The used model in TCAD simulation for the calculation of the I - V characteristics of organic TFTs explained in supplementary material.¹¹

In summary, for extracting the sub-bandgap DOS of polymer semiconductors, main backbones of printed electronics, the multi-frequency C - V spectroscopy is proposed and demonstrated for three different polymer (P3HT, PQT-12, and PQTBTz-C12) semiconductor-based organic TFTs. The extracted DOS is consistent with the polymer-dependence of the measured crystallinity and mobility. It was verified through the TCAD simulation comparing with the measured I - V characteristics. The proposed method does

not require a special preparation or complicated measurement setup (for the light illumination and/or thermal effects) and directly reflects the effects of DOS on the circuit performance because it uses the bias- and frequency-dependences of the small signal capacitance. Therefore, the multi-frequency C - V spectroscopy is expected to be potentially useful for the modeling, characterization, and circuit design of polymer-based organic TFTs.

This work was supported by the National Research Foundation of Korea (NRF) grant funded by the Ministry of Education, Science and Technology (MEST) (Grant No. 2011-0000313). The CAD software was supported by SIL-VACO and IC Design Education Center.

¹M. C. J. M. Vissenberg and M. Matters, *Phys. Rev. B* **57**, 12964 (1998).

²C. Krellner, S. Haas, C. Goldmann, K. P. Pernstich, D. J. Gundlach, and B. Batlogg, *Phys. Rev. B* **75**, 245115 (2007).

³T. Sueyoshi, H. Fukagawa, M. Ono, S. Kera, and N. Ueno, *Appl. Phys. Lett.* **95**, 183303 (2009).

⁴E. J. Meijer, M. Matters, P. T. Herwig, D. M. de Leeuw, and T. M. Klapwijk, *Appl. Phys. Lett.* **76**, 3433 (2000).

⁵K. Lee, M. S. Oh, S. Mun, K. H. Lee, T. W. Ha, J. H. Kim, S. K. Park, C. Hwang, B. H. Lee, M. M. Sung, and S. Im, *Adv. Mater.* **20**, 3260 (2010).

⁶W. L. Kalb and B. Batlogg, *Phys. Rev. B* **81**, 035327 (2010).

⁷B. S. Ong, Y. Wu, P. Liu, and S. Gardner, *J. Am. Chem. Soc.* **126**, 3378 (2004).

⁸D. H. Kim, B. L. Lee, H. Moon, H. M. Kang, E. J. Jeong, J. I. Park, K. M. Han, S. Lee, B. W. Yoo, B. W. Koo, J. Y. Kim, W. H. Lee, K. Cho, H. A. Becerril, and Z. Bao, *J. Am. Chem. Soc.* **131**, 6124 (2009).

⁹R. D. McCullough, *Adv. Mater.* **10**, 93 (1998).

¹⁰S. Lee, S. Park, S. Kim, Y. Jeon, K. Jeon, J.-H. Park, J. Park, I. Song, C. J. Kim, Y. Park, D. M. Kim, and D. H. Kim, *IEEE Electron Devices Lett.* **31**, 231 (2010).

¹¹See supplementary material at <http://dx.doi.org/10.1063/1.3698455> for the calculation of the I - V characteristics of organic TFTs.